Cave ice stable isotopes suggest summer temperatures in East-Central Europe link to AMO variability

Carmen-Andreea Bădăluță[1,2,3], Aurel Perșoiu[1,4], Monica Ionita[5], Natalia Piotrowska[6]

[1]Stable Isotope Laboratory, Ștefan cel Mare University, Suceava, 720229, Romania
[2]Department of Geography, Ștefan cel Mare University, Suceava, 720229, Romania
[3]Institute for Geological and Geochemical Research, Research Centre for Astronomy and Earth Sciences MTA, Budapest, 1112, Hungary
[4]Emil Racoviță Institute of Speleology, Romanian Academy, Cluj Napoca, 400006, Romania
[5]Alfred Wegener Institute, Helmholtz Center for Polar and Marine Research, Bremerhaven, 27515, Germany
[6]Institute of Physics, Silesian University of Technology, Gliwice, 44-100, Poland

Correspondence to: Carmen-A. Bădăluță (carmen.badaluta@usm.ro), Aurel Perșoiu (aurel.persoiu@gmail.com)

Abstract. The climate of East-Central Europe (ECE) is the result of a combination of influences originating in the wider North Atlantic realm, the Mediterranean Sea and Western Asia/Siberia. Climate models suggest that these competing influences will result in difficult to predict responses to ongoing climatic changes, thus making mitigation and adaptation strategies challenging to devise and implement. Previous studies have shown that the complex interplay between the large-scale atmospheric patterns across the region result in strongly dissimilar summer and winter conditions on time scales ranging from decades to millennia. To put these into a wider context, long term climate reconstructions are required, but, largely due to historical reasons, these are lacking in ECE. We address these issues by presenting a high resolution, precisely dated record of summer temperature variations during the last millennium in ECE based on the stable isotopic analysis of a 4.84 m ice core extracted from Focul Viu Ice Cave (Western Carpathians, Romania). The data shows little summer temperature differences between the Medieval Warm Period (MWP) and the Little Ice Age (LIA) on centennial scales, but well-expressed minima and maxima, which occurred synchronously with periods of low and high solar activity. Further, summer temperatures fluctuated with a periodicity similar to that of the Atlantic Multidecadal Oscillation suggesting that solar variability-induced climatic changes were transferred locally by atmospheric processes. Contrary to summer temperatures, winter ones show stronger contrasts between the MWP and LIA, thus suggesting that the later were likely an expression of winter climatic conditions.

1 Introduction

Rapid global warming (IPCC, 2018) and the ensuing suite of climatic changes that it triggers (Coumou and Rahmstorf, 2012) demand a clear understanding of the background mechanisms of climate change in order to be able to disentangle natural and anthropogenic processes (Haustein et al., 2017; IPCC, 2018). Particularly valuable are high-resolution reconstructions of the past variability of different climatic variables – seasonal air temperatures, precipitation levels, moisture sources – that allow direct comparisons with the dynamics of natural forcing and further deciphering the mechanisms of past and present climate changes. The last 1000 years are particularly significant as the European climate changed from generally warm, to cold (the Medieval Warm Period-Little Ice Age transition, Jones et al., 2009) and back to warm (the present-day warming, Neukom et al., 2019) conditions. These transitions allow the links between forcing and climatic response to be tested. While several global (Jones and Mann, 2004; Mann et al, 2009) and hemispheric (Moberg et al, 2005; Neukom et al., 2019; PAGES 2k Consortium, 2019; Ljungqvist et al., 2019) climatic reconstructions have been published, these made no seasonal differentiation – a task that recently became increasingly necessary to constrain seasonally distinctive climatic changes (e.g., Ljungqvist et al., 2019), as these respond to different forcing mechanisms (e.g., Perșoiu et al., 2019). On multidecadal time scales, summer climate over Europe is influenced mainly by the Atlantic Multidecadal Oscillation (AMO). The AMO is a

climate mode of variability associated with periodic anomalies of sea surface temperatures (SSTs) in northern, extratropical latitudes. The positive phase is characterized by positive SST anomalies spanning the whole North Atlantic Ocean and is associated with above normal temperature over the central and eastern part of Europe; the negative phase is characterized by negative SST anomalies over the North Atlantic Ocean and is associated with below normal temperatures over the central and eastern part of Europe. Over Europe the influence of the AMO is clearest during summer (Sutton and Dong, 2012; Ionița et al., 2012; 2017; O'Reilly et al., 2017).

In temperate climatic regions, one of the most sensitive environmental archives are ice caves (Homlund et al., 2005, Kern and Perșoiu, 2013), i.e., rock-caves hosting perennial accumulations of ice. In such caves, ice forms either by the freezing of water or direct snow deposition via entrance shafts (e.g., Mavlyudov, 2018). Several studies have shown that these deposits host a wealth of information on past climate variability. Thus, Perșoiu et al. (2017) and Sancho et al. (2018) have shown that proxies in cave ice forming during winter months record changes in temperature and moisture sources, likely influenced by the dynamics of the North Atlantic Oscillation. Other studies have used pollen and plant macrofossils recovered from cave ice to reconstruct past vegetation dynamics (Feurdean et al., 2011; Leunda et al., 2019) while others used the accumulation rate of ice as indicators of past climatic variability (e.g., Kern et al., 2018) or atmospheric processes (Kern et al., 2009). Studies of ice caves in southern Europe have also highlighted the sensitivity of cave glaciers to summer climatic conditions (Colucci et al., 2016; Colucci and Guglielmin, 2019; Perșoiu et al., 2020). Regardless of the deposition style, the ice records the original stable isotope composition of precipitation that further reflects changes in air temperature and thus is an important archive of past temperature and moisture source variability (Perșoiu et al., 2011a, 2011b). The Carpathian Mountains host several ice caves (Brad et al., 2018) that preserve a large variety of geochemical information on past climate and environmental changes (Fórizs et al., 2004; Kern et al., 2004; Citterio et al., 2005; Perșoiu et al., 2017). Here, we present a reconstruction of summer climate variability and large-scale circulation drivers during the last 1000 years in East Central Europe based on the $\delta^{18}O$ and $\delta^{2}H$ values measured along an ice core drilled in Focul Viu Ice Cave (Western Carpathian Mountains, Romania).

2 Site information

Focul Viu Ice Cave (FV, 107 m long, ~30 m deep) is located in the Central Bihor Mountains, Romania (46.27º N; 22.68º E, 1165 m above sea level, Fig. 1a, Perșoiu and Onac, 2019). The cave has a simple morphology (Fig. 1b, 1c) with a small entrance that opens into the Great Hall (68 × 46 m), which, in turn, is followed by a narrow gallery (Little Hall, 20 × 5 m). The ceiling of the Great Hall opens to the surface (Fig. 1c) allowing precipitation to reach the cave. Below the opening, and covering the entire surface of the Great Hall, a layered ice block has developed, with an estimated thickness of 20 m and minimum volume of 30,000 m^3 (Orghidan et al., 1984; Brad et al., 2018). The downward sloping morphology of the cave and the presence of the two openings determine air circulation (Perșoiu and Onac, 2019) with cold air inflow through the lower entrance and warm air outflow through the upper one in winter, and slow convective circulation within the cave (with no air mass exchange with the exterior) during summer. As a result of this air circulation, between October and April the dynamics of air temperature inside and outside of the cave follow a similar pattern while between May and September the cave's temperatures are stable at 0 °C.

A direct consequence of the predominantly negative air temperatures in the cave is the genesis, accumulation and preservation of ice (Fig. 1b, 1c). During summer, infiltrating rainwater accumulates on top of the existing ice block and at the onset of negative temperatures in September starts to freeze forming a 1-20 cm thick layer of ice. Infiltration and subsequent freezing of water during warm periods in winter results in additional layers of ice on top of the ice block. At the onset of melting in April/May, this winter ice melts. The result of these processes is a multiannual, layered, ice block, consisting of annual couplets of clear ice (on top) and a sediment-rich layer beneath. Inflow of warm water in wet summers

leads to rapid ablation of the ice at the top of the ice block, partly altering the annual layering. The processes of cave ice formation by water freezing and the registration of environmental signals by various proxies (e.g., stable isotope composition of ice, pollen content) have been described from the nearby Scărișoara Ice Cave (Perșoiu and Pazdur, 2011; Feurdean et al., 2011) and, given the similarities between the two caves, are also pertinent to Focul Viu Ice Cave. The one notable difference is the timing of the onset of freezing: in Scărișoara Ice Cave, the onset of freezing is delayed until late-autumn and early winter (Perșoiu et al., 2017), whereas in Focul Viu Ice Cave freezing starts in early autumn.

3 Methods

3.1 Drilling and stable isotope analyses

The FV ice core (4.87 m long, 10 cm diameter) was drilled in May 2016 from the Great Hall of FV Ice Cave (Fig. 1d) using a modified PICO electric drill (Koci and Kuivine, 1984) manufactured by Heavy Duties S.R.L (Cluj Napoca, Romania). The ice core was cut into 1 cm layers considering also the annual layering in a cold room, except for the section between 290 and 320 cm below surface, where we intercepted a tree trunk. Each sample was sealed in a plastic bag, allowed to melt at room temperature, transferred to a 20 mL HDPE scintillation vial and stored at 4 °C prior to analysis.

Precipitation samples were collected monthly between March 2012 and December 2018 at Gheţar (GT, 46°29'28.45" N, 22°49'26.02" E, 1100 m asl, ~15 km SE of the location of FV Cave) using collectors built according to IAEA specification.

Water samples were analyzed for stable isotope composition at the Stable Isotope Laboratory, Ștefan cel Mare University (Suceava, Romania), using a Picarro L2130*i* CRDS analyzer connected to a high precision vaporizing module. All samples were filtered through 0.45 μm nylon membranes before analysis and manually injected into the vaporization module multiple times, until the standard deviation of the last four injections was less than 0.03 for $\delta^{18}O$ and 0.3 for $\delta^{2}H$, respectively. The average of these last four injections was normalized on the SMOW-SLAP scale using two internal standards calibrated against VSMOW2 and SLAP2 standards provided by the IAEA and used in our interpretation. A third standard was used to check the long-term stability of the analyzer. The stable isotope composition of oxygen and hydrogen are reported using standard δ notation, with precision estimated to be better than 0.16 ‰ for $\delta^{18}O$ and 0.7 ‰ for $\delta^{2}H$ respectively, based on repeated measurements of an internal standard.

3.2 Radiocarbon dating and age-depth model construction

The wide opening to the surface in the ceiling of the Great Hall (Fig. 1c) allows for a large volume of organic matter to fall into the cave and subsequently become trapped in the ice. During drilling, we recovered over 40 samples of organic matter from large tree trunks to pieces of leaves. Only 14 were suitable for radiocarbon dating, of which 2 were not datable due to their extremely small carbon yield. AMS radiocarbon analyses were performed at the Institute of Physics, Silesian University of Technology, Gliwice, Poland (Piotrowska, 2013). All samples were precleaned with standard acid-alkali-acid treatment, dried and subjected to graphite preparation using an AGE-3 system (IonPlus, CH) equipped with an Elementar VarioMicroCube elemental analyzer and automated graphitization unit (Wacker et al., 2010; Nemec et al., 2010). The ^{14}C concentrations in graphite produced from unknown samples, Oxalic Acid II standards and coal blanks were measured by the DirectAMS laboratory, Bothell, USA (Zoppi et al., 2007). The results are reported in Table 1. The radiocarbon dates were calibrated using OxCal v4.3 (Bronk Ramsey, 2009) and the IntCal13 calibration curve (Reimer et al., 2013). The NH1 curve (Hua et al., 2013) was used for one post-bomb date.

Because organic material can fall into the cave decades to centuries before being trapped in the ice (see Fig. 1b), we have carefully screened the radiocarbon results prior to age-depth modeling with the aim of selecting the most reliable dates forming a chronological sequence and not contradict the previously well-dated core reported by Maggi et al. (2008). In total, four dates were selected for age-depth modeling. For the top of the ice core a uniform age distribution from 1991 to 2016

AD was assigned, allowing for the possibility of surface ice melting. The model was constructed using the OxCal *P_Sequence* algorithm (Bronk Ramsey, 2008) with variable prior *k* parameter (*k*=1, U (-2,2); Bronk Ramsey and Lee, 2013) and extrapolated to a depth of 4.86 m. The agreement index of the model was 85 %, confirming a good statistical performance when the threshold of 60 % is surpassed. The sections between the dated depths were assumed to have a constant deposition rate. The complete age-depth model is shown in Fig. 2. For further analysis the mean age derived from the model was used and is also reported in Table 1.

3.3 Climate data

The sea surface temperature (SST) is extracted from the Extended Reconstructed Sea Surface Temperature data (ERSSTv5) of Huang et al. (2018). This dataset covers the period 1854 – present and has a spatial resolution of 2° x 2°. The AMO index used in this study has been obtained from https://climexp.knmi.nl/data/iamo_ersst_ts.dat and is based also on the ERSSTv5 data set. The station-based meteorological data was provided by the Romanian National Meteorological Administration.

4 Results and discussions

4.1 Ice accumulation in Focul Viu Ice Cave

The results of the radiocarbon analyses performed on organic matter recovered from the ice are shown in Table 1 with the age-depth model shown in Fig. 2. The maximum age of the ice is 1000±20 cal BP at 4.45 m below surface based on direct dating of organic remains and 1100 cal BP at 4.86 m below surface (extrapolation). A rock embedded in the ice at 4.87 m below the surface blocked the drill, but previous work in the cave has shown that the thickness of the ice block exceeds 15 m (Orghidan et al., 1984; Kern et al., 2004; Perșoiu and Onac, 2019).

The ice accumulation rate was 0.39-0.41 cm/year between AD 850 and 950, 0.29-0.37 cm/year between AD 950 and AD 1000, 0.36-0.38 cm/year between AD 1010 and AD 1215, 0.4-0.44 cm/year between AD 1220 and AD 1970 and 0.56 cm/years over the past 40 years. The average for the entire ice core is 0.42 cm/year. The variability seen in the ice accumulation rate during the last 1000 years results from the variable processes involved in the growth and decay of cave ice. Ice can melt as a result of either warm summers with enhanced conductive heat transfer to the cave or wet summers, with rapid ablation resulting from water flowing across the top of the ice block. Subsequently, ice growth is influenced by the amount of water present at the onset of freezing, the timing of this onset and its duration. Thus, the resulting accumulation rate is a record of the complex interplay of these climatic conditions, being an indicator of both ice growth and melting. The high accumulation rates registered between AD 810 and AD 1230 were likely the result of greater amounts of water available in the cave during the generally wet conditions of the Medieval Warm Period (Feurdean et al., 2015). The highest accumulation rates were recorded between AD 1230 and AD 1400, a period of enhanced Mediterranean moisture transport to the site and slightly warmer winters compared to the preceding and ensuing periods. After AD 1400, palaeoclimate records from the region indicate an abrupt increase in summer precipitation of Atlantic origin (Feurdean et al., 2015) and a drop in winter temperature (Perșoiu et al., 2017) likely causing rapid and sustained summer melting and the early onset of freezing, thus resulting in an abrupt reduction of net ice accumulation. After AD 1450, the climate in the region was dominated by dry summers with frequent storms and cold winters (Perșoiu, 2017). These conditions lead to a reduction in the water available for freezing in early autumn and thus no winter ice accumulation, as well as enhanced summer melting; a combination of processes resulting in minimal ice accumulation.

4.2 Stable isotopes in Focul Viu cave ice - proxies for summer air temperatures and AMO variability

The variability of $\delta^{18}O$ and $\delta^{2}H$ in precipitation at Gheţar, 10 km south of the cave's location and at the same altitude and assessed for the 2012-2017 period, follows that of temperature (Fig. 3a) with the maximum values (-3.6 ‰ and -26 ‰, for

$\delta^{18}O$ and $\delta^{2}H$, respectively) in July/August and minimum (-19.8 ‰ and -140 ‰, for $\delta^{18}O$ and $\delta^{2}H$, respectively) in January. Similar results were found by Bojar et al. (2009) and Ersek et al. (2018) for the same region suggesting that the $^{18}O/^{16}O$ and $^{2}H/^{1}H$ ratios in precipitation register temperature changes on a regional scale. The Local Meteoric Water Line, defined by the equation $\delta^{18}O = 7.4*\delta^{2}H + 6.1$ (Fig. 3b) has a slope and intercept very similar to those found by Ersek et al (2018). Precipitation in the region is mainly delivered by weather systems carrying moisture from the Atlantic Ocean with the Mediterranean Sea contributing moisture during autumn and winter (Nagavciuc et al, 2019b). The deuterium excess in precipitation (*d-excess* or d), defined as $d = \delta^{2}H - 8*\delta^{18}O$ (Dansgaard, 1964), allows for a clear separation of the air masses: Atlantic ocean (d-excess close to the global average of 10 (Craig, 1961)) and the Mediterranean Sea (d-excess between 12 and 17, resulting from the high evaporative conditions in the Eastern Mediterranean Sea). Similarly high values of *d-excess* have been measured by Drăguşin et al. (2017) in precipitation in southwest Romania and Bădăluță et al. (2019) in precipitation in northeast Romania and linked to air masses originating in the strongly evaporated Mediterranean and Black seas, respectively.

The FV $\delta^{18}O_{ice}$ and $\delta^{2}H_{ice}$ records span the AD 850 – AD 2016 period showing generally stable values throughout the analyzed period on which decadal to multi-decadal scale oscillations are superimposed. Both records display a remarkable similarity throughout the entire period and in our discussion we have used only $\delta^{18}O$.

Observations on the dynamics of cave ice during the past 18 years have shown that it starts to grow in early autumn through the freezing of water accumulated during summer. As the ceiling of the cave is open to the surface, precipitation directly reaches the site of ice formation so that the stable isotope composition of precipitation is not modified in the epikarst above the cave, thus preserving the original $\delta^{18}O$ and $\delta^{2}H$ values of summer (June-July-August, JJA) precipitation. Further, $\delta^{18}O$ and $\delta^{2}H$ values in the FV ice core from the past 20 years are similar to values registered in the summer (JJA) precipitation at Gheţar (Fig. 3b) further supporting our inference that stable isotope values in cave ice preserve the summer climatic signal. However, while freezing processes in caves could alter the original $\delta^{18}O$ (and $\delta^{2}H$) values in cave ice, several studies have shown (e.g., in the nearby Scărişoara Ice Cave (Perşoiu et al. (2011b)) that the original climatic signal embedded in the stable isotope composition of cave ice is preserved and can be used as a proxy for external climate variability.

Overall, our observations of cave ice genesis and dynamics and stable isotope monitoring data clearly indicate that summer air temperatures are registered and preserved in the ice block in FV Cave. In order to test the long-term preservation of these connections, we have analyzed the links between the FV $\delta^{18}O_{ice}$ record and instrumental data from three nearby meteorological stations over the AD 1851 – AD 2016 period. On multidecadal time scales, summer air temperature changes in the region are controlled mainly by the dynamics of the Atlantic Multidecadal Oscillation (Ionita et al., 2012). Fig. 4. shows the JJA air temperature at Baia Mare (BM), Sibiu (SB) and Timişoara (TM) meteorological stations (all located in Romania, within 80 km of the location of Focul Viu Ice Cave), the AMO index and FV $\delta^{18}O_{ice}$. The instrumental temperature data indicates large multidecadal variability with a cold period between AD 1890 and AD 1920, followed by a warm period between AD 1921 and AD 1960, a slightly colder period between AD 1960 and AD 2000, and enhanced warming over the last two decades; all following the AMO variability. The $\delta^{18}O_{ice}$ values show a similar temporal evolution, the slight offsets between the observational data and $\delta^{18}O$ being likely due to the dating uncertainty (20 – 35 years). Further, we have computed the correlation map between the summer mean air temperature at SB station (with the longest instrumental record) and the summer SST as indicator of AMO variability (Sutton and Dong, 2012). To remove short-term variability and retain only the multidecadal signal in our data, prior to the correlation analysis, both the temperature time series and the SST data were smoothed with a 21-year running mean filter. Figure 5 clearly shows that positive (negative) temperature anomalies over the analyzed region are associated with positive (negative) SST anomalies over the North Atlantic Ocean, resembling the SST anomalies associated with the positive (negative) phase of AMO (Mesta-Nuñez and Enfield 1999, Latif et al. 2004;

Knight et al. 2005). These results are also in agreement with the results of Della-Marta et al. (2007), showing that extreme high temperatures over Europe are triggered, at least partially, by the phase of AMO. A recent study of $\delta^{18}O$ variability in oak tree rings in NW Romania (~50 km NW from our site) also indicates the influence of the AMO on summer temperatures and drought conditions (Nagavciuc et al., 2019a). A potential physical mechanisms for the multidecadal variability of $\delta^{18}O$ in our ice cave can be as follows: prolonged periods of positive temperature anomalies throughout the summer months related to prolonged warm SST in the North Atlantic Ocean, lead to high $\delta^{18}O$ values in the FV ice core via enhanced ice melting, while prolonged cold summers related to a cold North Atlantic Ocean, lead to low $\delta^{18}O$ values.

Combining all the data above, it results that on time scales ranging from years to decades, prolonged periods of positive temperature anomalies throughout the summer months, linked to prolonged warm SSTs in the North Atlantic Ocean (and thus a positive AMO index), could be preserved by the $\delta^{18}O_{ice}$ in FV Ice Cave. We have compared the FV $\delta^{18}O_{ice}$ with tree ring width (TRW) reconstruction of JJA temperature anomalies (Popa and Kern, 2009). The highest similarities between the FV ice core and TRW records were found for the cold periods between AD 1000 – 1050, 1250 – 1300, 1420 – 1680, 1750 – 1850 and 1960 – 1980 and the warm periods during AD 1080 – 1200, 1850 – 1960. In contrast, some differences have been identified during the period AD 1640 – 1740, when the TRW record indicated above-average summer temperatures while the $\delta^{18}O$ record shows low values which suggest below – average summer temperatures (Fig. 7). Given the very different nature of the two archives (trees versus cave ice), of the proxies (TRW and $\delta^{18}O$) and of the chronologies (annual tree ring counting vs. ^{14}C dating), the two records agree remarkably well, further supporting the hypothesis that $\delta^{18}O$ and $\delta^{2}H$ values in FV ice core is registering both summer air temperature variability during the past ca. 1000 years in East-Central Europe, as well as, on a broader spatial scale, the variability of the AMO.

Similar to the AD 1850-2016 interval described above, the stable isotope record closely mirrors the AMO variability over the entire studied interval (Fig. 6), suggesting a possible link between summer temperatures in Eastern Europe and solar influence. The relationship between the FV $\delta^{18}O_{ice}$ and AMO records is strongest between ~AD 1750 and AD 2016 and between AD 1125 and AD 1525, with decadal-scale variability in the two records being synchronous within the dating uncertainty (i.e., less than 30 years lag).

The apparent ~50 yrs lag of the FV $\delta^{18}O_{ice}$ record behind the AMO between AD 1600 and AD 1775 could have resulted from 1) high (> 50 years) uncertainty between AD 1525 and AD 1750, as well as before AD 1125 (Fig. 7a); 2) uncertainties in the reconstruction of AMO indexes before the instrumental record. Kilbourne et al. (2013) have shown, by comparing different proxy records of the AMO, that there is no consensus yet on the history of Atlantic multidecadal variability. Despite the similarities during the instrumental period, all the records they used in their study are quite different during the pre-instrumental era, most likely due to a lack of available well-dated, high-resolution marine proxy temperature records; 3) a less-straightforward link between solar forcing and the AMO (Knudsen et al., 2014) during the LIA. However, we do see the apparent breakdown of the correlation between summer temperatures and AMO only for a short period between AD 1600 and 1750 as well as around AD 1050, periods when our chronology has the highest uncertainties. Further, the overall succession of high and low $\delta^{18}O$ values mimics the changes seen in the AMO reconstruction, so that the discrepancies could be the result of these uncertainties. If so, the record presented here suggest that solar-induced changes in the North Atlantic are transferred, likely *via* atmospheric processes, towards the wider Northern Hemisphere, resulting in hemispheric-wide climatic responses to perturbations in the North Atlantic

Several periods of excursions towards low $\delta^{18}O$ values (suggesting low summer temperatures) dot the past 1100 years (Fig. 7), the most notable one being around AD 870-930, AD 1045-1080, AD 1270-1325, AD 1430-1475, AD 1525-1550, AD 1715-1730, AD 1820-1865 and AD 1880-1925. Significant maxima occurred between AD 850-875, AD 1010-1030, AD 1350-1390, AD 1485-1510, AD 1625-1695 and AD 1950-1970. All these minima and maxima, except for the one centered on AD 1840 coincide (Fig. 7) with the known solar minima and maxima of the past 1000 years (the Spörer Minimum

between AD 1450 and AD 1550 is split in two in our record, by a brief interval of possibly high temperatures around AD 1500, similarly to the other records from Europe).

The FV $\delta^{18}O_{ice}$ record is in agreement with other summer temperature reconstructions (e.g., Buntgen et al., 2011) at regional and hemispheric scale (Fig. 7). Further, regional summer temperature (e.g., Popa and Kern, 2009) and summer temperature-sensitive drought (Seim et al., 2012) reconstructions show warm peaks around AD 1320, 1420, 1560, 1780 and cooling around AD 1260, 1450 and 1820, similar with reconstructions and models at global level (Neukom et al., 2019) and the FV temperature reconstruction (this study). Contrary to the summer season temperature reconstructions, a late-autumn through early winter season temperature reconstructions from the nearby Scărișoara Ice Cave (Perșoiu et al., 2017) shows that the MWP was rather warm and also wet (Feurdean et al., 2011), while the LIA was cold, and likely drier and with erratically distributed precipitation. Together, these data suggest a complex picture of climate variability in the wider Carpathian region, with much of the yearly temperature variability during the past 1000 years being attributed to the influence of winter conditions, summer temperatures being rather constant. On this long-term trend, brief "excursions" were likely the result of large-scale circulation influences, with solar variability induced changes being transferred locally by atmospheric processes.

5 Conclusions

The analysis of the oxygen and hydrogen stable isotope ratios along a ~5 m long ice core extracted from Focul Viu Ice Cave (northwest Romania) provides an unprecedented view on the dynamics of summer air temperature and atmospheric circulation changes during the last 1000 years in the poorly investigated region of East-Central Europe. The data show little millennial-scale summer temperature variability since the onset of the Medieval Warm Period and through the Little Ice Age. Nevertheless, well-expressed minima and maxima occurred synchronously with periods of low and high solar activity possibly suggesting a causal mechanism. Similarly, decadal-scale summer temperature variability follows that of the Atlantic Multidecadal Oscillation and we subsequently hypothesize that solar-induced changes in summer climatic conditions over the Northern Atlantic are transferred through atmospheric processes across the Northern Hemisphere. Further evidence in similar records is required to test this hypothesis. Contrary to summer temperatures, winter ones show a stronger contrast between the Medieval Warm Period and the Little Ice Age, thus suggesting that the later were likely an expression of winter climatic conditions.

Author contributions. CAB and AP designed the project, AP and CAB collected the ice core and CAB performed the stable isotope analyses. NP performed the radiocarbon analyses and constructed the depth-age model. MI analyzed the climate and large-scale circulation data. CBD and AP wrote the text, with input from MI and NP.

Competing interests. The authors declare that they have no conflict of interest.

Data availability. The Focul Viu $\delta^{18}O$ and $\delta^{2}H$, as well as the ^{14}C data and the modeled ages will be made available upon publication both on the CP webpage and on the NOAA/World Data Service for Paleoclimatology webpage. The meteorological data plotted in figure 4 was provided by the Romanian National Meteorological Administration, except for the AMO data (panel a) which was downloaded from https://climexp.knmi.nl/data/iamo_ersst_ts.dat. The paleoclimate data used to plot fig. 7, panels a, b, c, d and e was downloaded from the NOAA/World Data Service for Paleoclimatology webpage.

Acknowledgments. The research leading to these results has received funding from EEA Financial Mechanism 2009- 2014 under the project contract no CLIMFOR18SEE. AP was partial financially supported by UEFISCDI Romania through grants no. PN-III-P1-1.1-TE-2016-2210 and PNII-RU-TE-2014-4-1993. MI was partially supported by the AWI Strategy Fund Project PalEX and by the Polar Regions and Coasts in the Changing Earth System (PACES) program of the AWI. We thank the Administration of the Apuseni National Park for granting permission to drill in Focul Viu Ice Cave, Nicodim Pașca for collecting precipitation samples, dr. Christian Ciubotărescu for help during the ice core drilling effort and Vlad Murariu (Heavy Duties Romania) for developing and constructing the drilling equipment. We thank the editor and two anonymous reviewers for comments that helped us improve the original manuscript and Simon M. Hutchinson (University of Salford, UK) and Sara Asha Burgess for language corrections.

Financial support. The article processing charges for this open-access publication were covered by the project EXCALIBUR of the Ștefan cel Mare University of Suceava, Romania.

References

Bădăluță, C.–A.**,** Persoiu, A., Ionita, M., Nagavciuc, V., and Bistricean, P. I.: Stable H and O isotope-based investigation of moisture sources and their role in river and groundwater recharge in the NE Carpathian Mountains, East-Central Europe, Isot. Environ. Healt. S., 55 (2), 161–178, https://doi.org/10.1080/10256016.2019.1588895, 2019.

Brad, T., Bădăluță C.-A., and Persoiu, A.: Ice caves in Romania, in: Ice caves, edited by: Perșoiu, A. and Lauritzen, S.-E., Elsevier, Amsterdam, Netherlands, 511–528, https://doi.org/10.1016/B978-0-12-811739-2.00025-5, 2018.

Bojar, A, Ottner, F, Bojar, H. P., Grigorescu, D., and Persoiu, A.: Stable isotope and mineralogical investigations on clays from the Late Cretaceous sequences, Hațeg Basin, Romania, Appl. Clay Sci., 45, 155–163, https://doi.org/10.1016/j.clay.2009.04.005, 2009.

Bronk Ramsey, C. and Lee, S.: Recent and Planned Developments of the Program OxCal, Radiocarbon, 55, 720–730, https://doi.org/10.1017/S0033822200057878, 2013.

Bronk Ramsey, C.: Bayesian analysis of radiocarbon dates, Radiocarbon, 51, 337–360, 2009.

Bronk Ramsey, C.: Deposition models for chronological records, Quaternary Sci. Rev., 27, 42–60, https://doi.org/10.1016/j.quascirev.2007.01.019, 2008.

Büntgen, U., Tegel, W., Nicolussi, K., McCormick, M., Frank, D., Trouet, V., Kaplan, J. O., Herzig, F., Heussner, K-U., Wanner, H., Luterbacher, J., and Esper, J.: 2500 Years of European Climate Variability and Human Susceptibility, Science, 331, 578–582, https://doi.org/10.1126/science.1197175, 2011.

Citterio, M., Turri, S., Perșoiu, A., Bini, A., and Maggi, V.: Radiocarbon ages from two ice caves in the Italian Alps and the Romanian Carpathians and their significance, In: Glacier Caves and Glacial Karst in High Mountains and Polar Regions, edited by: Mavlyudov, B. R., Institute of geography of the Russian Academy of Sciences, Moscow, Russia, 87–92, 2005.

Colucci, R. R., and Guglielmin, M.: Climate change and rapid ice melt: Suggestions from abrupt permafrost degradation and ice melting in an alpine ice cave, Progress in Physical Geography: Earth and Environment, 43, 561-573, 10.1177/0309133319846056, 2019.

Colucci, R. R., Fontana, D., Forte, E., Potleca, M., and Guglielmin, M.: Response of ice caves to weather extremes in the southeastern Alps, Europe, Geomorphology, 261, 1-11, http://dx.doi.org/10.1016/j.geomorph.2016.02.017, 2016.

Coumou, D., and Rahmstorf, S.: A decade of weather extremes, Nat. Clim. Change, 2, 491–496, https://doi.org/10.1038/nclimate1452, 2012.

Craig, H.: Isotopic variations in meteoric waters, Science, 133, 1702–1703, https://doi.org/10.1126/science.133.3465.1702, 1961.

D'Arrigo, R., Wilson, R., and Jacoby G.: On the long-term context for late twentieth century warming, J. Geophys. Res., 111, D03103, https://doi.org/10.1029/2005JD006352, 2006.

Dansgaard, W.: Stable isotope in precipitation, Tellus, 16, 436–438, https://doi.org/10.1111/j.2153-3490.1964.tb00181.x, 1964.

Della-Marta, P. M., Luterbacher, J., von Weissenfluh, H., Xoplaki, E., Brunet, M., and Wanner, H.: Summer heat waves over western Europe 1880–2003, their relationship to large scale forcings and predictability, Clim. Dynam., 29, 251–275, https://doi.org/10.1007/s00382-007-0233-1, 2007.

Dragusin, V., Balan, S., Blamart, D., Forray, F. L., Marin, C., Mirea, I., Nagavciuc, V., Persoiu, A., Tirla, L., Tudorache, A., and Vlaicu, M.: Transfer of environmental signals from surface to the underground at Ascunsă Cave, Romania, Hydrol. Earth Syst. Sci., 21, 5357–5373, https://doi.org/10.5194/hess-21-5357-2017, 2017.

Feurdean, A., Persoiu, A., Pazdur, A., and Onac, B. P.: Evaluating the palaeoecological potential of pollen recovered from ice in caves: a case study from Scarisoara Ice Cave, Romania, Rev. Palaeobot. Palyno., 165, 1–10, https://doi.org/10.1016/j.revpalbo.2011.01.007, 2011.

Feurdean, A., Galka, M, Kuske, E., Tanțău, I., Lamentowicz, M., Florescu, G., Liakka, J., Hutchinson, S. M., Mulch, A., and Hickler, T.: Last Millennium hydro-climate variability in Central Eastern Europe (Northern Carpathians, Romania), Holocene, 25, 1179–1192, https://doi.org/10.1177/0959683615580197, 2015.

Fórizs, I., Kern, Z., Szántó, Zs., Nagy, B., Palcsu, L., Molnár, M.: Environmental isotopes study on perennial ice in the Focul Viu Ice Cave, Bihor Mountains, Romania. Theor. App. Karst.17, 61–69, 2004.

Haustein, K., Allen, M. R., Forster, P. M., Otto, F. E. L., Mitchell, D. M., Matthews, H. D., and Frame, D. J.: A real-time Global Warming Index, Sci. Rep., 7: 15417, https://doi.org/10.1038/s41598-017-14828-5, 2017.

Holmlund, P., Onac, B. P., Hansson, M., Holmgren, K., Morth, M., Nyman, M., and Persoiu, A.: Assessing the palaeoclimate potential of cave glaciers: the example of the Scărișoara Ice Cave (Romania), Geogr. Ann. A, 87A, 193–201, https://doi.org/10.1111/j.0435-3676.2005.00252.x, 2005.

Hua, Q., Barbetti, M., and Rakowski, A. Z.: Atmospheric Radiocarbon for the Period 1950–2010, Radiocarbon, 55, 2059–2072, https://doi.org/10.2458/azu_js_rc.v55i2.1, 2013.

Huang, B., Angel, W., Boyer, T., Cheng, L., Chepurin, G., Freeman, E., Liu, C., and Zhang, H.-M.: Evaluating SST analyses with independent ocean profile observations, J. Climate, 31, 5015–5030, https://doi.org/10.1175/JCLI-D-17-0824.1, 2018.

IPCC: Global warming of 1.5°C. An IPCC Special Report. Geneva, Switzerland, https://doi.org/10.1017/CBO9781107415324, 2018.

Ionita, M., Rimbu, N., Chelcea, S., and Patrut, S.: Multidecadal variability of summer temperature over Romania and its relation with Atlantic Multidecadal Oscillation, Theor. Appl. Climatol., 113, 305–315, https://doi.org/10.1007/s00704-012-0786-8, 2012.

Jones, P. D., Osborn, T. J., and Briffa, K. R.: The evolution of climate over the last millennium, Science, 292(5517), 662-667, https://doi.org/10.1126/science.1059126, 2001.

Jones, P. D., and Mann, M. E.: Climate over the past millennia, Rev. Geophys., 42, RG2002, https://doi.org/10.1029/2003RG000143, 2004.

Jones, P. D., Briffa, K. R., Osborn, T. J., Lough, J. M., van Ommen, T. D., Vinther, B. M., Luterbacher, J., Wahl, E. R., Zwiers, F. W., Mann, M. E., Schmidt, G. A., Ammann, C. M., Buckley, B. M., Cobb, K. M., Esper, J., Goosse, H., Graham, N., Jansen, E., Kiefer, T., Kull, C., Küttel, M., Mosley-Thompson, E., Overpeck, J. T., Riedwyl, N., Schulz, M., Tudhope, A. W., Villalba, R., Wanner, H., Wolff, E., and Xoplaki, E.: High-resolution palaeoclimatology of the last millennium: A review of current status and future prospects, The Holocene, 19, 3–49, https://doi.org/10.1177/0959683608098952, 2009.

Kern, Z., and Persoiu, A.: Cave ice - the imminent loss of untapped mid-latitude cryospheric palaeoenvironmental archives, Quaternary Sci. Rev., 67, 1-7, https://doi.org/10.1016/j.quascirev.2013.01.008, 2013.

Kern, Z., Fórizs, I., Nagy, B., Kázmér, M., Gál, A., Szánto, Z., Palcsu, L., and Molnár, M.: Late Holocene environmental changes recorded at Gheţarul de la Focul Viu, Bihor Mountains, Romania, Theor. App. Karst., 17, 51–60, 2004.

Kern, Z., Molnár, M., Svingor, É., Persoiu, A., and Nagy, B.: High-resolution, well-preserved tritium record in the ice of Bortig Ice Cave, Bihor Mountains, Romania, The Holocene, 19, 729-736, https://doi.org/10.1177/0959683609105296, 2009.

Kern, Z., Bočić, N., and Sipos, G.: Radiocarbon-Dated Vegetal Remains from the Cave Ice Deposits of Velebit Mountain, Croatia, Radiocarbon, 60, 1391-1402, https://doi.org/10.1017/RDC.2018.108, 2018.

Kilbourne, K. H., Alexander, M. A., and Nye, J. A.: A low latitude paleoclimate perspective on Atlantic multidecadal variability, J. Marine Syst., 133, 4–13, https://doi.org/10.1016/j.jmarsys.2013.09.004, 2013.

Knight, J. R., Allan, R. J., Folland, C. K., Vellinga, M., and Mann, M.E.: A signature of persistent natural thermohaline circulation cycles in observed climate, Geophys. Res. Lett., 32, L20708, https://doi.org/10.1029/2005GL024233, 2005.

Knudsen, M. F., Jacobsen B. H., Seidenkrantz, M.-S., and Olsen, J.: Evidence for external forcing of the Atlantic Multidecadal Oscillation since termination of the Little Ice Age, Nat. Commun., 5: 3323, https://doi.org/10.1038/ncomms4323, 2014.

Koci, B. R., and Kuivinen, K. C.: The PICO lightweight coring auger, J. Glaciol., 30, 244–245, https://doi.org/10.3189/S0022143000006018, 1984.

Latif, M., Botset, E. R. M., Esch, M., Haak, H., Hagemann, S., Jungclaus, J., Legutke, S., Marsland, S., and Mikolajewicz, U.: Reconstructing, monitoring and predicting multidecadal-scale changes in the North Atlantic thermohaline circulation with sea surface temperature, J. Climate, 17, 1605–1614, https://doi.org/10.1175/1520-0442(2004)017<1605:RMAPMC>2.0.CO;2, 2004.

Leunda, M., González-Sampériz, P., Gil-Romera, G., Bartolomé, M., Belmonte-Ribas, Á., Gómez-García, D., Kaltenrieder, P., Rubiales, J. M., Schwörer, C., Tinner, W., Morales-Molino, C., and Sancho, C.: Ice cave reveals environmental forcing of long-term Pyrenean tree line dynamics, J. Ecol., 107, 814-828, https://doi.org/10.1111/1365-2745.13077, 2019.

Ljungqvist, F. C., Seim, A., Krusic, P. J., González-Rouco, J. F., Werner, J. P., Cook, E. R., Zorita, E., Luterbacher, J., Xoplaki, E., Destouni, G., García-Bustamante, E., Aguilar, C. A. M., Seftigen, K., Wang, J., Gagen, M. H., Esper, J., Solomina, O., Fleitmann, D., and Büntgen, U.: European warm-season temperature and hydroclimate since 850 CE, Environ. Res. Lett., 14, 084015, https://doi.org/10.1088/1748-9326/ab2c7e, 2019.

Maggi, V., Turri, S., Bini, A., and Udisti, R.: 2500 Years of history in Focul Viu Ice Cave, Romania, In: Proceedings of the 3rd International Workshop on Ice Caves, edited by: Kadebskaya, O., Mavlyudov, B., and Patunin, M., Kungur Ice Cave, Russia, 11–15, 2008.

Mann, M. E., Zhang, Z., Rutherford, S., Bradley, R., Hughes, M. K., Shindell, D., Ammann, C., Faluvegi, G., and Ni, F.: Global signatures and dynamical origins of the Little Ice Age and Medieval Climate Anomaly, Science, 326, 1256–1260, https://doi.org/10.1126/science.117730, 2009.

Mavlyudov, B. R.: Ice genesis and types of ice caves, in: Ice caves, edited by: Perșoiu, A. and Lauritzen, S. E., 34-68, https://doi.org/10.1016/B978-0-12-811739-2.00032-2, 2018.

Mesta-Nuñez, A. M., and Enfield, D. B.: Rotated global modes of non-ENSO sea surface temperature variability, J. Climate, 12, 2734–2746, https://doi.org/10.1175/1520-0442(1999)012<2734:RGMONE>2.0.CO;2, 1999.

Moberg, A., Sonechkin, D. M., Holmgren, K., Datsenko, N. M. and Karlén, W.: Highly variable Northern Hemisphere temperatures reconstructed from low- and high-resolution proxy data, Nature, 433, 613-617, https://doi.org/10.1038/nature03265, 2005.

Nagavciuc V., Bădăluță C.-A., Ionita M.: Tracing the Relationship between Precipitation and River Water in the Northern Carpathians Base on the Evaluation of Water Isotope Data, Geosciences, 9, 198; https://doi.org/10.3390/geosciences9050198, 2019.

Nagavciuc, V., Ionita, M., Persoiu, A., Popa, I., Loader, N. J., and McCarroll, D.: Stable oxygen isotopes in Romanian oak tree rings record summer droughts and associated large-scale circulation patterns over Europe, Clim. Dynam., 52, 6557–6568, https://doi.org/10.1007/s00382-018-4530-7, 2019a.

Nemec, M., Wacker, L., and Gäggeler, H. W.: Optimization of the Graphitization Process at AGE-1, Radiocarbon, 52, 1380–1393, 2010.

Neukom, R., Steiger, N., Gómez-Navarro, J.J., Wang, J. and Werner, J. P.: No evidence for globally coherent warm and cold periods over the preindustrial Common Era, Nature, 571, 550–554, https://doi.org/10.1038/s41586-019-1401-2, 2019.

Orghidan, T., Negrea, Ş., Racoviță, G., and Lascu, C.: Peşteri din România: ghid turistic. Ed. Sport-Turism, Bucureşti, 1984.

O'Reilly, C. H., Woollings, T., and Zanna, L.: The Dynamical Influence of the Atlantic Multidecadal Oscillation on Continental Climate, J. Climate, 30, 7213–7230, https://doi.org/10.1175/JCLI-D-16-0345.1, 2017.

PAGES 2K Consortium: Consistent multidecadal variability in global temperature reconstructions and simulations over the Common Era, Nat. Geosci., 12, 643–649, https://doi.org/10.1038/s41561-019-0400-0, 2019.

Persoiu, A.: Climate evolution during the Late Glacial and the Holocene. In: Landform dynamics and evolution in Romania, edited by: Rădoane, M., and Vespremeanu-Stroe, A., Springer, Berlin, Heidelberg, Germany, 57–66. https://doi.org/10.1007/978-3-319-32589-7_3, 2017.

Persoiu, A., and Pazdur, A: Ice genesis and its long-term dynamics in Scărișoara Ice Cave, Romania, The Cryosphere, 5, 45–53, https://doi.org/0.5194/tc-5-45-2011, 2011.

Persoiu, A., and Onac, B. P.: Ice caves in Romania, In: Cave and Karst Systems of Romania, edited by: Ponta, G. M. L., and Onac, B. P., Springer, Berlin, Heidelberg, Germany, 455–465, https://doi.org/10.1007/978-3-319-90747-5_52, 2019.

Persoiu, A., Onac, B. P., and Perșoiu, I.: The interplay between air temperature and ice dynamics in Scărișoara Ice Cave, Romania. Acta Carsologica, 40, 445–456, https://doi.org/10.3986/ac.v40i3.4, 2011a.

Persoiu, A., Onac, B. P., Wynn, J. G., Bojar, A.-V., and Holmgren, K.: Stable isotope behavior during cave ice formation by water freezing in Scărişoara Ice Cave, Romania, J. Geophys. Res., 116, D02111, https://doi.org/10.1029/2010JD014477, 2011b.

Persoiu, A, Onac, B. P., Wynn, J. G., Blaauw, M., Ionita, M., and Hansson, M.: Holocene winter climate variability in Central and Eastern Europe, Sci. Rep., 7: 1196, https://doi.org/10.1038/s41598-017-01397-w, 2017.

Persoiu, A., Ionita, M., and Weiss H.: Atmospheric blocking induced by the strengthened Siberian High led to drying in the Middle East during the 4.2 ka event –a hypothesis, Clim. Past, 15, 781–793, https://doi.org/10.5194/cp-2018-161, 2019.

Persoiu, A., Buzjak, N., Onaca, A., Pennos, C., Sotiriadis, Y., Ionita, M., Zachariadis, S., Kosutnik, J., Hegyi, A., and Butorac, V.: Accelerated loss of surface and cave ice in SE Europe related to heavy summer rains, The Cryosphere, under review.

Piotrowska, N.: Status report of AMS sample preparation laboratory at GADAM Centre, Gliwice, Poland, Nuclear Instruments and Methods in Physics Research Section B, 294, 176–181, 2013.

Popa, I., and Kern, Z.: Long-Term Summer Temperature Reconstruction Inferred from Tree-ring Records from the Eastern Carpathians, Clim. Dyn., 32, 1107–1117, https://doi.org/10.1007/s00382-008-0439-x, 2009.

Reimer, P. J., Bard, E., Bayliss, A., Beck, J. W., Blackwell, P. G., Bronk Ramsey, C., Grootes, P. M., Guilderson, T. P., Haflidason, H., Hajdas, I., Hatte, C., Heaton, T. J., Hoffmann, D. L., Hogg, A. G., Hughen, K. A., Kaiser, K. F., Kromer, B., Manning, S. W., Niu, M., Reimer, R. W., Richards, D. A., Scott, E. M., Southon, J. R., Staff, R. A., Turney, C. S. M., and van der Plicht J.: IntCal13 and Marine13 Radiocarbon Age Calibration Curves 0-50,000 Years cal BP, Radiocarbon, 55, 1869–1887, https://doi.org/10.2458/azu_js_rc.55.16947, 2013.

Sancho, C., Belmonte, Á., Bartolomé, M., Moreno, A., Leunda, M., and López-Martínez, J.: Middle-to-late Holocene palaeoenvironmental reconstruction from the A294 ice-cave record (Central Pyrenees, northern Spain), Earth Planet. Sci. Lett., 484, 135-144, https://doi.org/10.1016/j.epsl.2017.12.027, 2018.

Seim, A., Büntgen, U., Fonti, P., Haska, H., Herzig, F., Tegel, W., Trouet, V., and Treydte, K.: Climate sensitivity of a millennium-long pine chronology from Albania, Clim. Res., 51, 217–228, https://doi.org/10.3354/cr01076, 2012.

Steinhilber, F., Beer, J., and Fröhlich, C.: Total solar irradiance during the Holocene, Geophys. Res. Lett., 36, L19704, https://doi.org/10.1029/2009GL040142, 2009.

Sutton, R. T., and Dong, B.: Atlantic Ocean influence on a shift in European climate in the 1990s, Nat. Geosci., 5, 788–792, https://doi.org/10.1038/ngeo1595, 2012.

Wacker, L., Nemec, M., and Bourquin, J.: A revolutionary graphitisation system: Fully automated, compact and simple, Nucl. Instrum. Meth. B, 268 (7-8), 931–934, 2010.

Wang, J., Yang, B., Ljungqvist, F. C., Luterbacher, J., Osborn, T.J., Briffa, K. R., and Zorita, E.: Internal and external forcing of multidecadal Atlantic climate variability over the past 1,200 years, Nat. Geosci., 10, 512–517, https://doi.org/10.1038/ngeo2962, 2017.

Zoppi, U., Crye, J., Song, Q., and Arjomand A.: Performance evaluation of the new AMS system at Accium BioSciences, Radiocarbon, 49, 173–182, 2007.

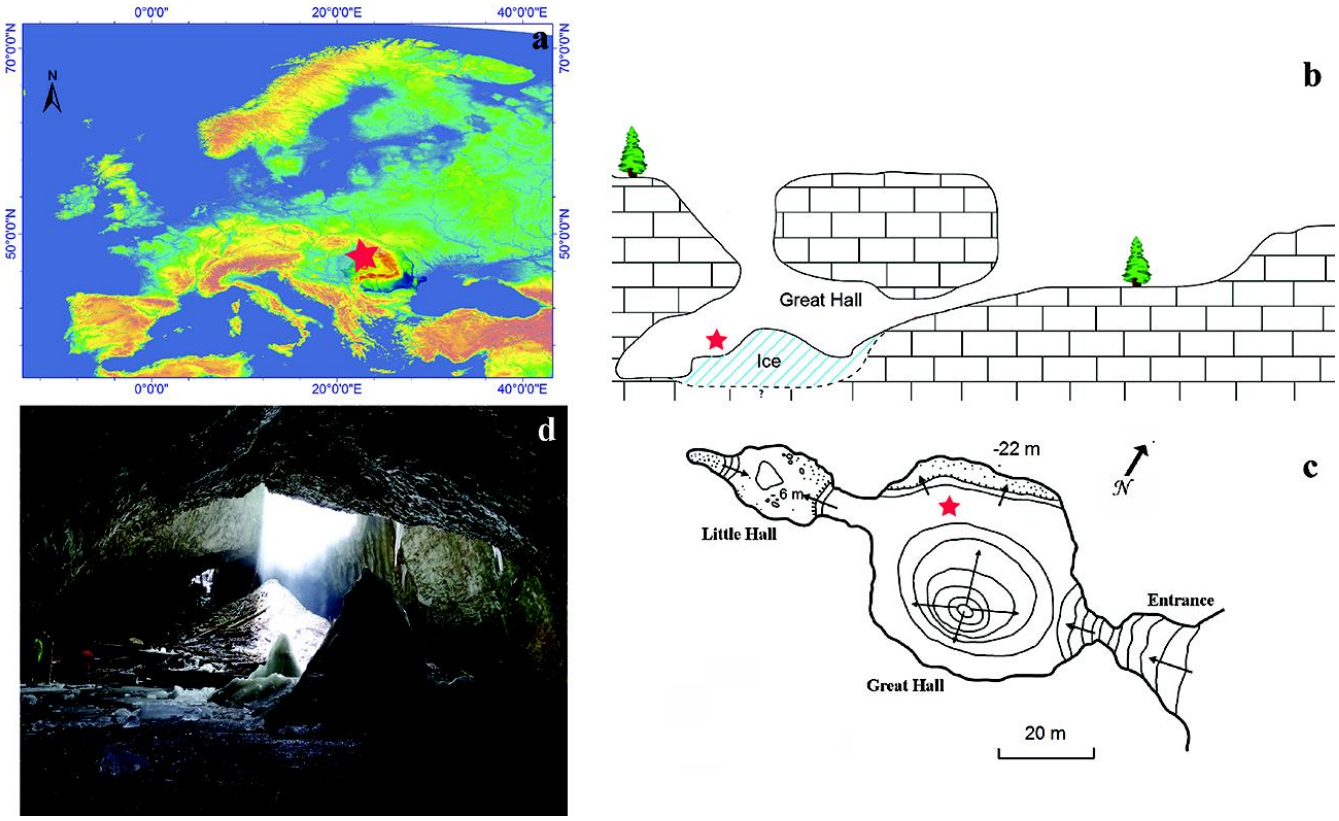

Figure 1. Location of the Focul Viu Ice Cave (red star) in Europe (a) cross section (b) and map (c) of the cave (red star indicates the drilling site) and (d) general view of the Great Hall (person in yellow on the far left is standing at the drilling site). The scale of the map and cross section are similar.

5

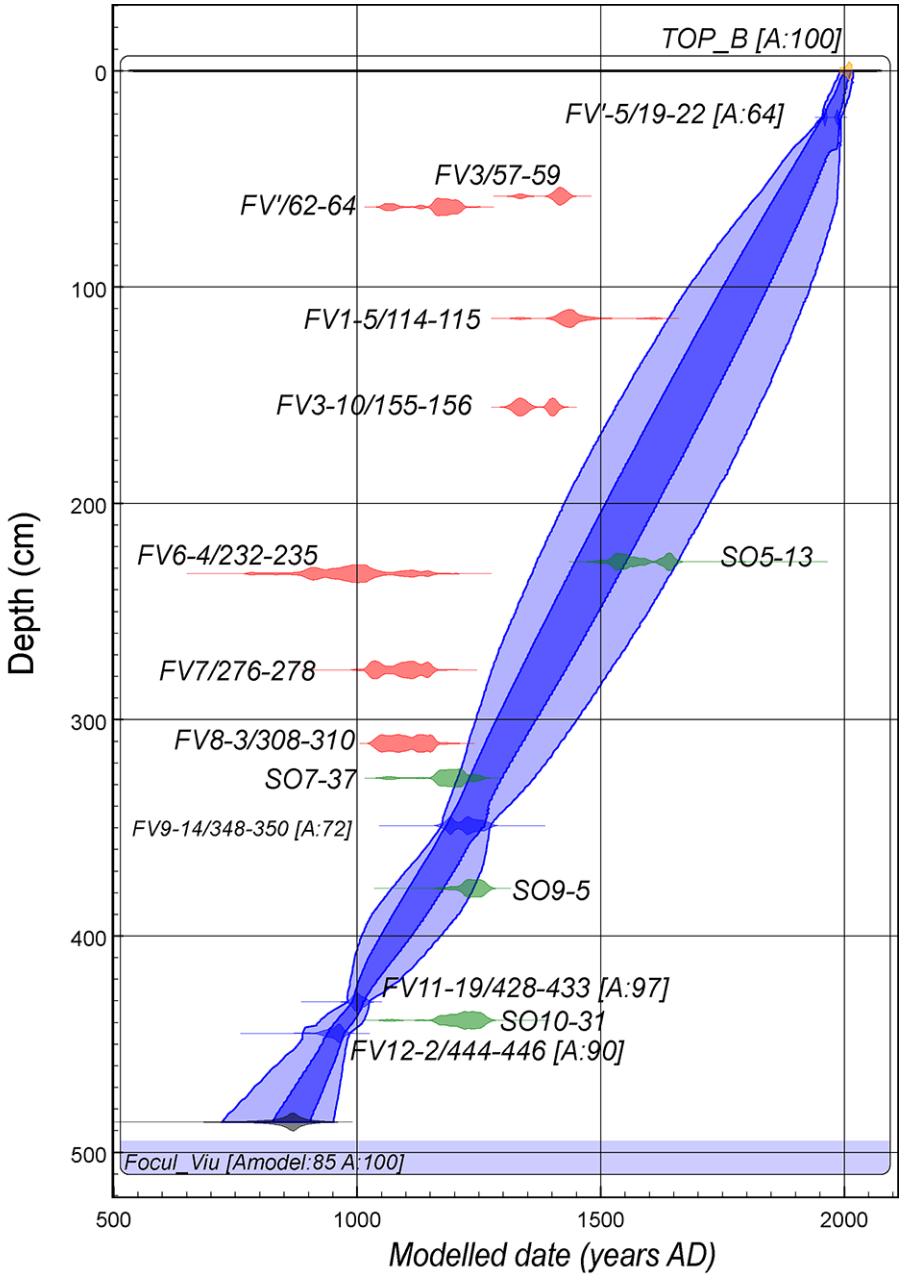

Figure 2. Age-depth model of the Focul Viu ice core. The calibrated age range of samples used in the model is indicated in blue and for those rejected in red. Samples in green are from the ice core drilled in 2004 (Maggi et al., 2008).

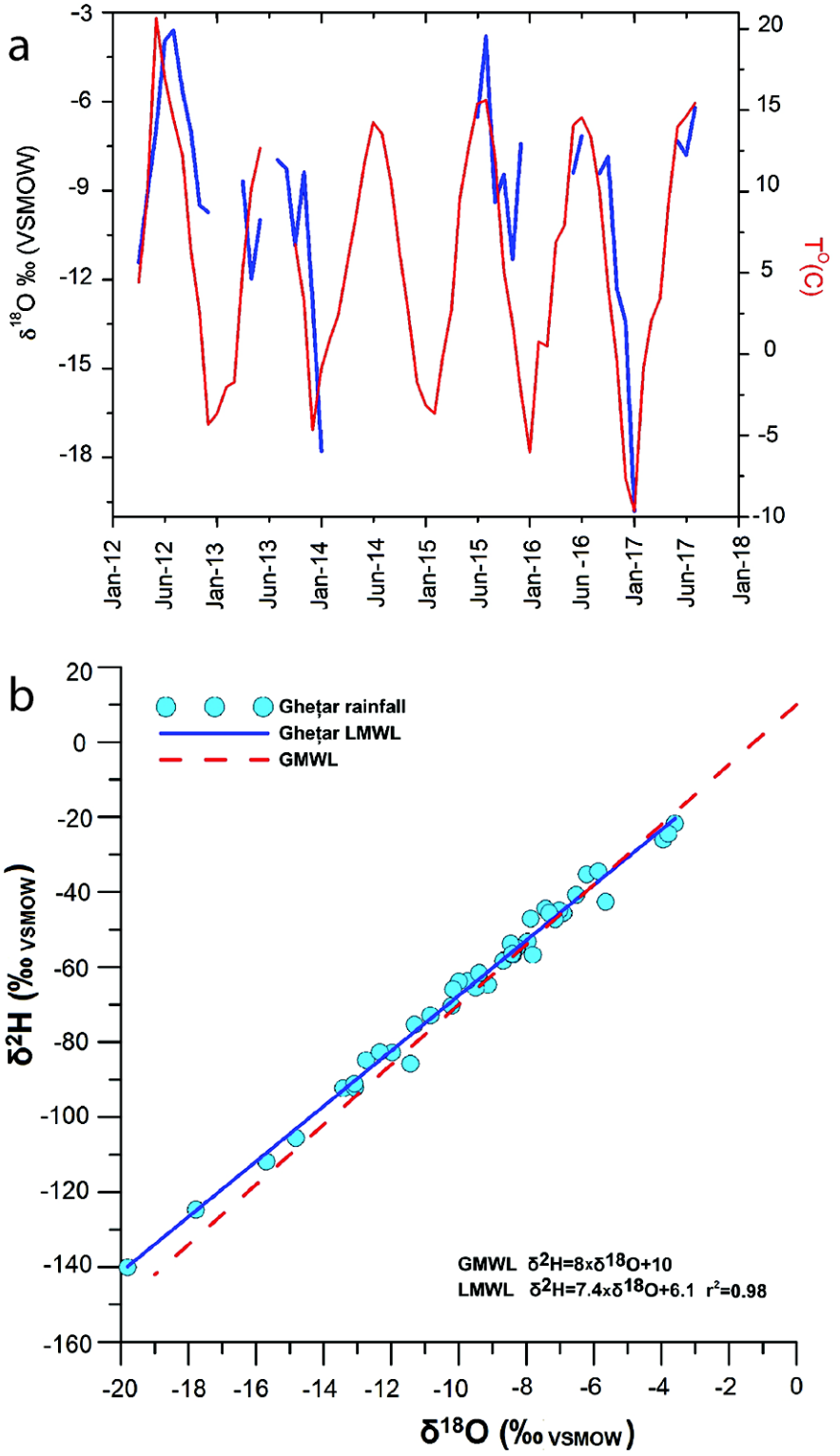

Figure 3. a) Temporal variability of $\delta^{18}O$ and $\delta^{2}H$ in precipitation and air temperature at Gheţar (10 km south of Focul Viu Ice Cave and at the same altitude), b) Local Meteoric Water Line of precipitation the same station plotted against the Global Meteoric Water Line

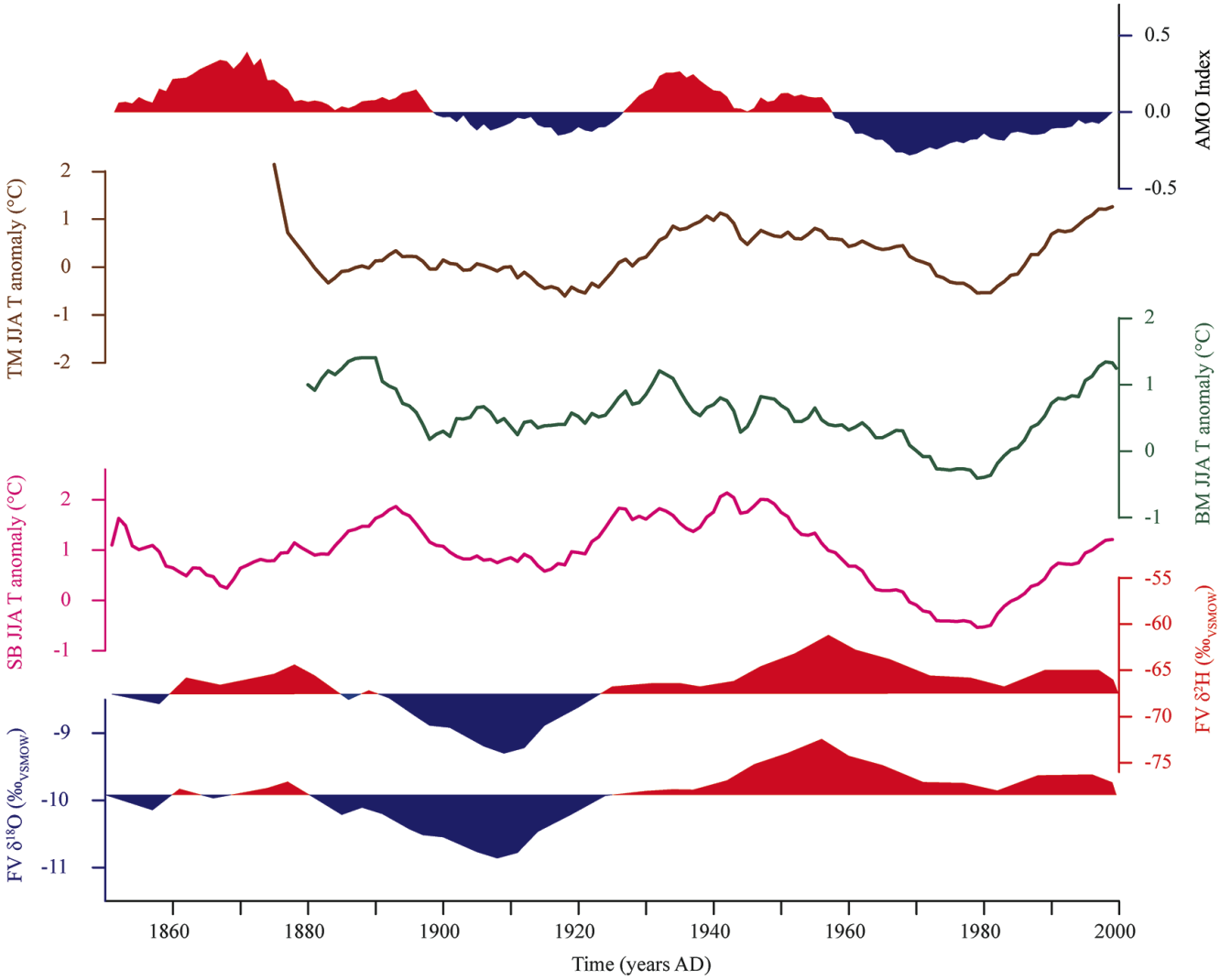

Figure 4. Temporal variability of the Atlantic Multidecadal Oscillation instrumental index, air temperature (anomalies with respect to the 1961-1990 period) recorded at Baia Mare (BM), Timişoara (TM) and Sibiu (SB) meteorological stations and FV $\delta^{18}O$ and $\delta^{2}H$ (‰) during the instrumental period. The positive (red) and negative (blue) anomalies are shown against the 1850-2000 averages for the FV δ values.

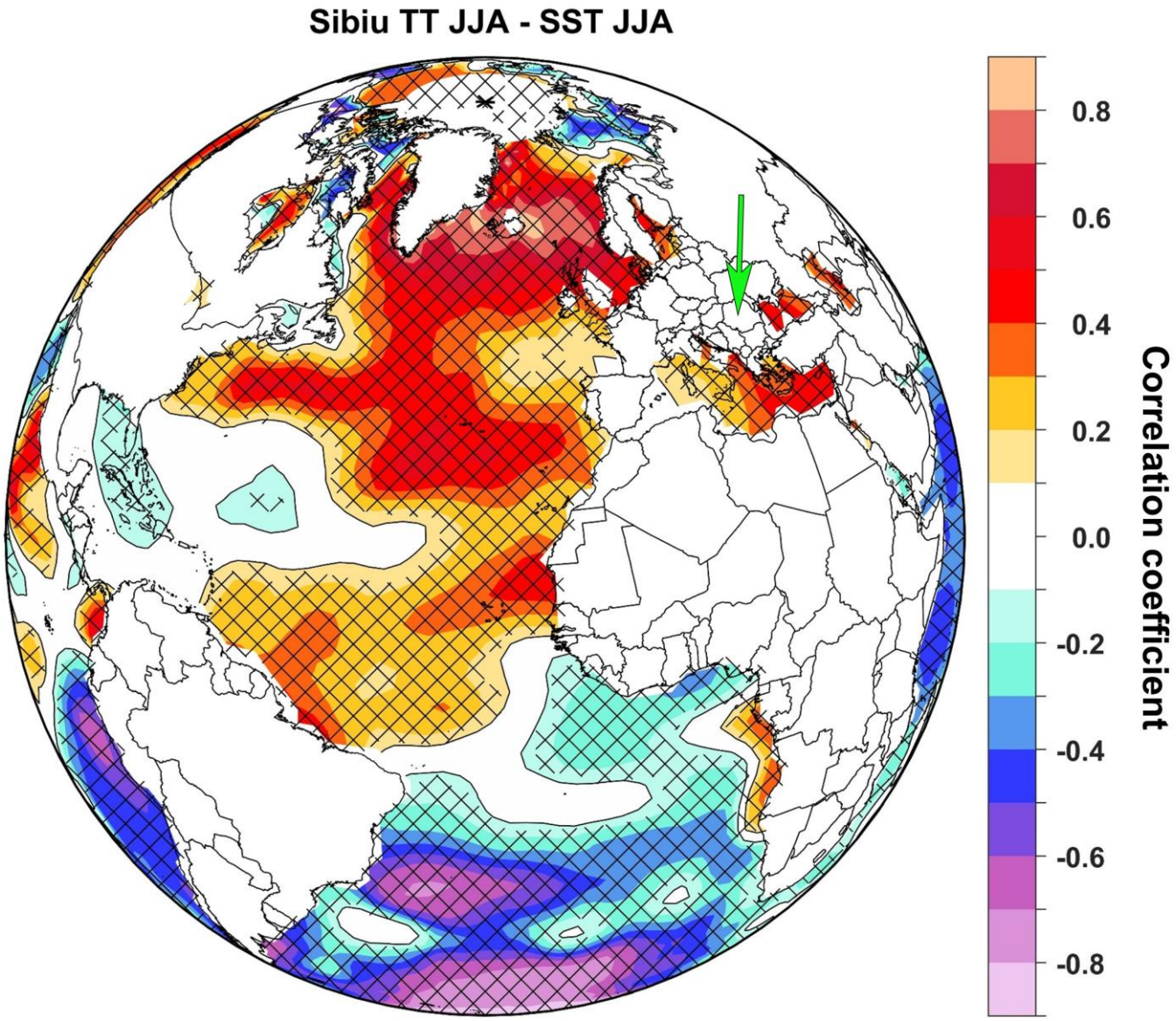

Figure 5. Spatial correlation map between Sea Surface Temperature (SST) and average summer (JJA June – July- August) air temperature at Sibiu (60 km south of Focul Viu Ice Cave indicated by the green arrow) over the 1850-2011 period.

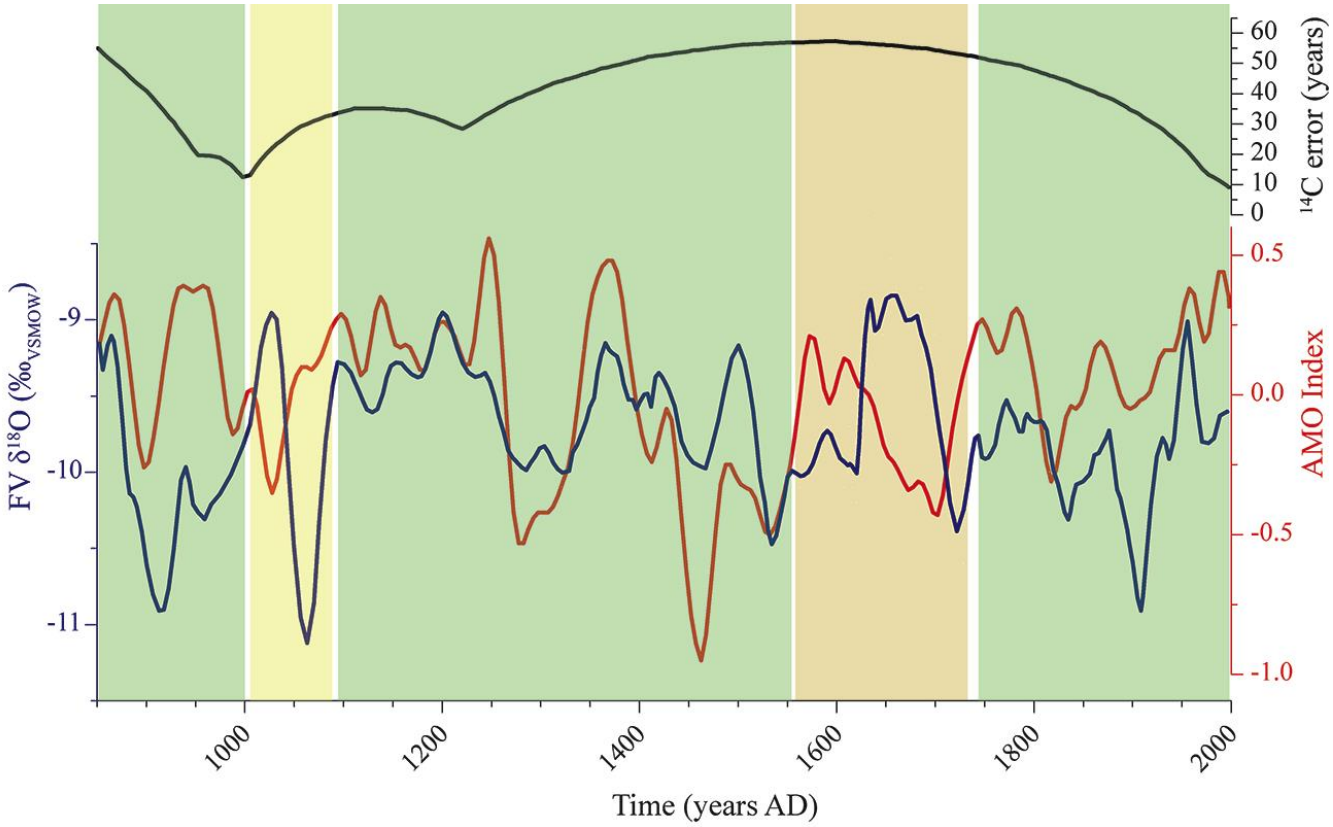

Figure 6. Temporal variability of the FV $\delta^{18}O$ (blue), the reconstructed AMO index (Wang et al., 2017) and the ^{14}C measurement uncertainty between AD 850 and 2000. Shading indicates the offset (in years) between the FV $\delta^{18}O$ and AMO index values: green – less than 20 years, yellow – between 20 and 50 years, orange – above 50 years.

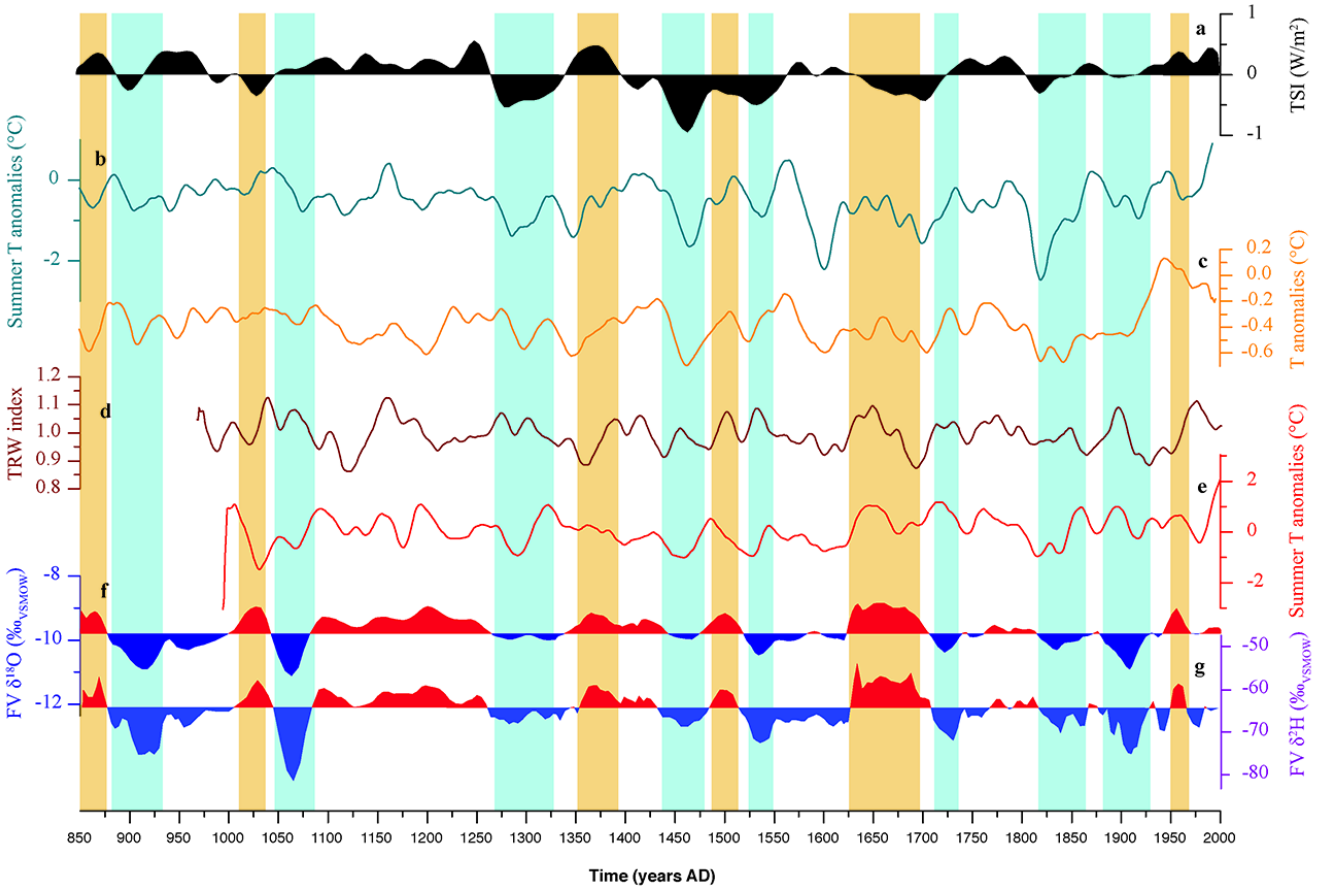

Figure 7. Summer climatic conditions recorded by $\delta^{18}O$ and $\delta^{2}H$ from FV ice core (panels f and g, bottom) and comparison with proxy indicator from the Northern Hemisphere: a) Total Solar Radiation (Steinhilber et al., 2009), b) Central Europe summer temperature anomalies (against the 1901-2000 mean, Buntgen et al., 2011); c) Northern Hemisphere air temperature anomalies (against the 1961-1990 mean, D'Arrigo et al., 2006), d) Tree Ring width index from Albania, SE Europe (Seim et al., 2012), e) Summer temperature anomalies in Romania (against the 1961-1990 mean, Popa and Kern, 2009).

Table 1. Radiocarbon data from the Focul Viu Ice Cave. Agreement indices for individual samples based on *P_Sequence* algorithm (Bronk Ramsey, 2008) are provided for accepted dates. Modeled ages for all dated depths are given as mean and sigma values, rounded to the nearest 5.

No	Lab code GdA-	Sample name	Depth (cm)	Material	Graphite mass (mg)	^{14}C age (BP)	Status and agreement index	Calibrated age ranges, unmodeled (AD)	Modeled age mean (AD) and 1 sigma
1	4889	FV'-5/19-22	21.5	needles and leaves, small fragments	0.86	-1410±25	Accepted (A=64%)	68.2% probability 1985AD (68.2%) 1988AD 95.4% probability 1958AD (9.6%) 1959AD 1985AD (85.8%) 1988AD	1975±20
2	5084	FV3/57-59	58	leaf fragments	0.54	525±30	Rejected	68.2% probability 1400AD (68.2%) 1435AD 95.4% probability 1320AD (14.9%) 1350AD 1390AD (80.5%) 1445AD	1890±45
3	4890	FV'/62-64	63	large wood fragment	1.00	875±25	Rejected	68.2% probability 1150AD (68.2%) 1215AD 95.4% probability 1045AD (18.1%) 1095AD 1120AD (4.6%) 1140AD 1145AD (72.7%) 1225AD	1880±45
4	5085	FV15/114-115	114.5	needle fragment, small	0.25	470±50	Rejected	68.2% probability 1405AD (68.2%) 1465AD 95.4% probability 1320AD (4.8%) 1350AD 1390AD (87.1%) 1520AD 1595AD (3.5%) 1620AD	1760±60
5	4891	FV3-10/155-156	155.5	small wood fragment	0.61	570±25	Rejected	68.2% probability 1320AD (40.2%) 1350AD 1390AD (28.0%) 1410AD 95.4% probability 1305AD (57.6%) 1365AD 1385AD (37.8%) 1420AD	1665±65
6	5086	FV6-4/232-235	232.5	needles and leaves, small fragments	0.14	1045±70	Rejected	68.2% probability 890AD (68.2%) 1040AD 95.4% probability 780AD (1.3%) 795AD	1490±65

								805AD (2.6%) 845AD 860AD (91.5%) 1160AD	
7	4892	FV7/276-278	277	large wood fragment	0.99	960±35	Rejected	68.2% probability 1020AD (22.4%) 1050AD 1080AD (34.5%) 1125AD 1135AD (11.3%) 1150AD 95.4% probability 1015AD (95.4%) 1160AD	1390±60
8	5087	FV8-3/308-310	311	small plant fragments	0.90	925±25	Rejected	68.2% probability 1040AD (42.8%) 1100AD 1120AD (25.4%) 1155AD 95.4% probability 1030AD (95.4%) 1165AD	1310±50
9	4893	FV9-14/348-350	349	leaves, fragments	0.99	780±35	Accepted (A=72%)	68.2% probability 1220AD (68.2%) 1270AD 95.4% probability 1190AD (95.4%) 1285AD	1225±30
10	5089	FV11-19/428-433	430.5	small plant fragments	0.61	1030±20	Accepted (A=97%)	68.2% probability 990AD (68.2%) 1020AD 95.4% probability 980AD (95.4%) 1030AD	1000±15
11	5090	FV12-2/444-446	445	small plant fragments	0.41	1140±20	Accepted (A=90%)	68.2% probability 885AD (19.7%) 905AD 915AD (48.5%) 965AD 95.4% probability 775AD (3.1%) 790AD 805AD (1.1%) 820AD 825AD (2.3%) 845AD 860AD (88.9%) 980AD	950±25